

Lasers and Synergetics

A Colloquium on Coherence and
Self-organization in Nature

Editors: R. Graham and A. Wunderlin

With 114 Figures

Springer-Verlag Berlin Heidelberg New York
London Paris Tokyo

Professor Dr. Robert Graham

Fachbereich 7, Universitäts-Gesamthochschule, Postfach 103764,
D-4300 Essen, Fed. Rep. of Germany

Dr. Arne Wunderlin

Institut für Theor. Physik, Universität, Pfaffenwaldring 57/IV,
D-7000 Stuttgart 80, Fed. Rep. of Germany

ISBN 3-540-17940-2 Springer-Verlag Berlin Heidelberg New York
ISBN 0-387-17940-2 Springer-Verlag New York Berlin Heidelberg

Library of Congress Cataloging-in-Publication Data. Lasers and synergetics. (Springer proceedings in physics; 19) "Extended versions of the contributions to a symposium in honour of the 60th birthday of Hermann Haken to be held in 1987 at the University of Stuttgart" – Pref. Includes index. 1. Lasers – Congresses. 2. System theory – Congresses. 3. Coherence (Optics) – Congresses. 4. Self-organizing systems – Congresses. 5. Haken, H. I. Graham, R. (Robert), 1942 –. II. Wunderlin, A. (Arne), 1947 –. III. Haken, H. IV. Series. QC685.L36 1987 535.5'8 87–12135

This work is subject to copyright. All rights are reserved, whether the whole or part of the material is concerned, specifically the rights of translation, reprinting, reuse of illustrations, recitation, broadcasting, reproduction on microfilms or in other ways, and storage in data banks. Duplication of this publication or parts thereof is only permitted under the provisions of the German Copyright Law of September 9, 1965, in its version of June 24, 1985, and a copyright fee must always be paid. Violations fall under the prosecution act of the German Copyright Law.

© Springer-Verlag Berlin Heidelberg 1987
Printed in Germany

The use of registered names, trademarks, etc. in this publication does not imply, even in the absence of a specific statement, that such names are exempt from the relevant protective laws and regulations and therefore free for general use.

Offset printing: Weihert-Druck GmbH, D-6100 Darmstadt
Bookbinding: J. Schäffer GmbH & Co. KG., D-6718 Grünstadt
2153/3150-543210

Contents

Part I Introduction

Contributions of Hermann Haken to Our Understanding of Coherence and Selforganization in Nature. By R. Graham 2

Part II Instabilities in Lasers

Laser Physics: Yesterday and Today
By F.T. Arecchi (With 4 Figures) 14

Recent Advances in Laser Instabilities. By L.A. Lugiato,
L.M. Narducci, D.K. Bandy, J.R. Tredicce, and P. Ru
(With 14 Figures) 24

Instabilities, Spatial and Temporal Patterns in Passive Optical
Systems
By L.A. Lugiato, L.M. Narducci, and R. Lefever (With 11 Figures) 53

Optical Instabilities in Semiconductors
By H. Haug (With 13 Figures) 72

Part III Fluctuations in Quantum Optics

The Polarization Symmetric Laser
By S. Großmann and W. Krauth (With 6 Figures) 90

Decay of Unstable Equilibria. By F. Haake (With 3 Figures) 99

Part IV After-Dinner Speech

Synergetics and Weltanschauung. By G. Caglioti (With 8 Figures) 112

Part V Methods of Synergetics

Boltzmann-Gibbs Entropy as a Measure of Order in Self-Organizing
(Synergetic) Systems. By Yu.L. Klimontovich 126

On the Slaving Principle. By A. Wunderlin	140
Solutions of Fokker-Planck Equations in Terms of Matrix Continued Fractions. By H. Risken (With 8 Figures)	148

Part VI Coherence and Structure in Physical Systems

Ultrafast Coherent Raman Spectroscopy By W. Zinth and W. Kaiser (With 6 Figures)	166
Coherence in the Transport of a Quantum Particle By P. Reineker and K. Kassner (With 4 Figures)	175
Structure Formation in Polymer Systems By G. Strobl (With 13 Figures)	191

Part VII Selforganization in Biological Systems

A General Approach to Complex Systems in Bioholonics By H. Shimizu (With 8 Figures)	204
Toward a Physical (Synergetic) Theory of Biological Coordination By J.A.S. Kelso and G. Schöner (With 4 Figures)	224
Synergetics and Social Science. By W. Weidlich (With 12 Figures)	238
Hermann Haken's Publications	257
Index of Contributors	271

Ultrafast Coherent Raman Spectroscopy

W. Zinth and W. Kaiser

Physik Department E11, Technische Universität München,
D-8000 München, Fed. Rep. of Germany

1. Introduction

During the past decade, time resolved coherent methods have attracted much interest for the study of fast dynamic processes. In particular, time resolved coherent Raman scattering allowed to measure - in the time domain - rapid dephasing processes of molecular vibrations in liquids and elucidated various line-broadening mechanisms /1-4/. It is the aim of this paper to focus attention on two more recent subjects. While time resolved Raman scattering is a method working in the time domain, it allows to obtain valuable information in the frequency domain /5,6/. The results of coherent experiments in the time domain have to be transformed by appropriate methods, e.g. by Fourier transformation, to show properties of the investigated system in the frequency domain. We present here two different approaches to relate time and frequency domain: (i) A time resolved coherent Raman experiment is performed and the spectrum of the coherently scattered light is recorded. (ii) A numerical transformation is applied to coherent data of high time resolution giving precise values of frequency differences of vibrational modes separated by several terahertz. Both techniques give - when applied in an appropriate way - results superior to steady-state spontaneous spectroscopy.

After a short theoretical description of the basic ideas of the two techniques we give experimental results. Measurements are presented where congested spectral regions consisting of several overlapping bands are resolved and the vibrational transition frequencies of the different components are determined. We also show that terahertz quantum beats can be measured with advanced experimental systems; they give precise values for the frequency differences between vibrational transitions separated by more than 200 cm^{-1} .

2. Theory

Time resolved coherent Raman scattering is commonly treated under the following assumptions /1/: Light fields are described by Maxwell's equation and the vibrational transitions are represented by two-level systems. Changes in the population of the two molecular levels are neglected (weak Raman interaction). Important is the coherent amplitude $\langle q \rangle$, i.e. the expectation value of the vibrational amplitude. First we discuss a single homogeneously broadened transition with dephasing time T_2 . We use the ansatz of plane waves for the coherent amplitude $\langle q \rangle = (i/2)Q \exp(-i\omega_q t + ik_q x) + \text{c.c.}$ and assume an isotropic Raman tensor for the investigated vibration. The coherent amplitude of a Raman active mode at frequency ω_q is excited via transient stimulated Raman scattering by a pair of light pulses, the laser pulse E_L and the Stokes pulse E_S /1,7/. The electric fields are considered to be plane waves, e.g. $E_L = 1/2 E_L \exp(-i\omega_L t + ik_L x) + \text{c.c.}$ with the wave vector k_L

and frequency ω_L for the laser field. The driving force $F(x,t)$ for the coherent amplitude Q is proportional to the product of the laser and the Stokes field, $F(x,t) \propto E_L E_S^*$; as a result the carrier frequency of the excitation force is $\omega_L - \omega_S$. The linear response theory applied to the excitation process leads to the following equation for the coherent amplitude Q :

$$Q(t) = \kappa \int_{-\infty}^t dt' E_L(t') E_S^*(t') \exp[(t'-t)/T_2 - i\Delta\omega t'] \quad (1)$$

The constant κ is defined in Ref./1/ and contains material parameters such as Raman cross section and vibrational frequency ω_q . T_2 stands for the dephasing time of the transition. Detuning between excitation frequency and vibrational mode is given by $\Delta\omega = \omega_L - \omega_S - \omega_q$. The coherent amplitude $\langle q \rangle$ under the action of a short exciting force evolves as follows: $\langle q \rangle$ rises to a maximum with the exciting force and, subsequently, decays exponentially with the dephasing time T_2 . During the free exponential decay the molecules oscillate at their resonance frequency ω_q . In the experiments described here, the large bandwidth of the short driving force allows to excite several vibrational modes simultaneously. The additional modes may be treated with the same ansatz, introducing the individual resonance frequencies ω_{qj} , amplitudes Q_j , and phase factors ϕ_j .

In a time resolved coherent Raman experiment the amplitude $\langle q \rangle$, generated at time zero, is monitored by coherent Raman scattering of a delayed probing pulse E_{L2} . We investigate the anti-Stokes part of the spectrum, which is generated by the nonlinear polarisation P^{NL}_{AS} :

$$P^{NL}_{AS} = \gamma \langle q \rangle E_{L2} + \chi^{(3)}_{NR} E_L E_S^* E_{L2} \quad (2)$$

The coherent signal consists of two parts. The first part on the r.h.s. of Eq.(2) describes the coherent Raman signal scattered from the excited vibrational mode. The constant γ contains the Raman cross section of the mode. This part of the coherent signal is emitted at the resonant anti-Stokes frequency $\omega_{AS} = \omega_{L2} + \omega_q$ and contains information on the dynamic properties of the investigated mode. The second part on the r.h.s. of Eq.(2) is caused by the nonresonant nonlinear susceptibility $\chi^{(3)}_{NR}$, which is related to off-resonant modes and electronic contributions. Especially distant electronic transitions determine this signal /8/. The nonresonant part of the signal gives an instantaneous response, i.e. it follows the product $E_L E_S^* E_{L2}$ and decays very rapidly with the time resolution of the experiment. The resonant part, on the other hand, shows the slower response of the resonantly excited mode. The nonresonant part of the coherent signal does not provide any information on the investigated modes. It has to be separated from the resonant signal. This fact is not possible in the steady-state coherent anti-Stokes Raman spectroscopy (CARS). In the time-resolved coherent anti-Stokes experiments described here the separation is possible. Measuring at later delay times allows to obtain information on the resonant part of the signal alone, while the nonresonant part has vanished at that time.

The two time-resolved spectroscopic techniques discussed next apply the same transient excitation process, but differ in the way the probing process is performed.

2.1 Short Excitation and Prolonged Interrogation spectroscopy

We introduce the so-called short excitation prolonged interrogation (SEPI) spectroscopy. Performing this technique one uses a short and

broad-band excitation process followed - at later delay times - by a coherent scattering process using a long probing pulse /5,9-11/. The frequency spectrum of the coherently scattered signal is detected. In order to gain optimum spectral resolution, a long and possibly Gaussian shaped probing pulse E_{L2} interrogates the coherent material excitation at a late delay time t_0 after the peak of the exciting force. At that time the coherent amplitude decays exponentially and the nonresonant contribution to the coherent signal $\chi^{(3)}_{NR}$ has disappeared. The anti-Stokes spectrum becomes

$$S_{AS}(\Omega) \propto |E_{AS}(\Omega)|^2$$

$$\propto \left| \int_{-\infty}^{+\infty} dt e^{i\Omega t} E_{AS}(t) \right|^2 = \left| \int_{-\infty}^{+\infty} dt e^{i(\Omega - \omega_{L2} - \omega_q)t} E_{L2}(t) Q(t) \right|^2. \quad (3)$$

The anti-Stokes signal is centered at the anti-Stokes frequency $\omega_A = \omega_{L2} + \omega_q$, provided that the probing light field does not exhibit phase modulation. Eq.(3) represents the Fourier transform of the product (probing field E_{L2} times the coherent amplitude Q), i.e. the Fourier transform of the product of a Gaussian function times an exponential function. This product is again a Gaussian function of the same width, which is shifted in time. In other words, the width of the anti-Stokes spectrum is determined by the Gaussian shape of the probing field E_{L2} , which may become very narrow provided one works with long (i.e. spectrally narrow) probing pulses. When the probing pulses are sufficiently long, $t_p > 1.4T_2$, the observed SEPI line is narrower than the spontaneous Raman band with $\Delta\nu_{spont} = 1/\pi T_2$. As a consequence, the anti-Stokes frequency may be determined with high accuracy. Of special interest is the application of the SEPI technique to congested spectral regions made up of overlapping vibrational bands. In this case, the narrowing of the different transitions below the spontaneous width allows to resolve individual transitions buried under a broad inhomogeneous spectrum.

2.2 Fourier Transform Raman Spectroscopy

In a second approach we record the coherent signal for a long time period in a pure time-domain experiment. In order to have optimum temporal resolution pulses of very short duration for the exciting and probing laser fields are required. Under these conditions the experiment detects the time-integrated coherent signal as a function of the delay time between exciting and probing process:

$$S(t_D) \propto \int_{-\infty}^{+\infty} dt |E_{AS}(t, t_D)|^2$$

$$\propto \int_{-\infty}^{+\infty} dt |P^{NL}_{AS}(t, t_D)|^2 = \int_{-\infty}^{+\infty} dt |\gamma\langle q \rangle E_{L2} + \chi^{(3)}_{NR} E_{L2} E_{L2}^* E_{L2}|^2. \quad (4)$$

For short exciting and probing pulses this experiment measures the component due to $\chi^{(3)}_{NR}$ at time zero and, most important, the time dependence of the coherent amplitude. When several modes are excited simultaneously, the signal decay is complex. It contains contributions of the different vibrational modes. It can be shown that for short driving and probing pulses the coherent signal is equivalent to the absolute square of the Fourier transform of the spontaneous Raman spectrum /5,6/. As a consequence, frequency domain information may be obtained from time resolved data by Fourier transformation.

The two techniques introduced here analyze the molecular system in a similar way. In the Fourier-transform spectroscopy the manipulation of the measured data prior to the transformation may lead to improved spectral resolution. In the SEPI experiment the handling of the information starts with the prolonged probing process using Gaussian shaped pulses. In this way, the exponential decay of the signal due to the dephasing process - corresponding to the homogeneous Lorentzian line shape in spontaneous spectroscopy - is removed prior to the spectral analysis. This procedure is equivalent to a numerical filtering of the time resolved data in the Fourier transform Raman spectroscopy /6/.

3. The Experimental System

An experimental set-up used successfully in various coherent Raman investigations is depicted schematically in Fig.1. A pumping laser source generates synchronized exciting and probing light fields at the frequencies ω_L , ω_{L2} , and ω_S in several dye lasers. The durations of the various laser pulses are determined by the special type of the laser. For the SEPI experiment we use a picosecond (synchronously pumped) dye laser emitting pulses E_L and E_{L2} with $\omega_L = \omega_{L2}$ of duration $t_p \approx 12$ ps and a second picosecond dye laser (pumped by the same mode-locked Ar-ion laser) to produce the Stokes pulse E_S ($t_p \approx 5$ ps) /12/. For the

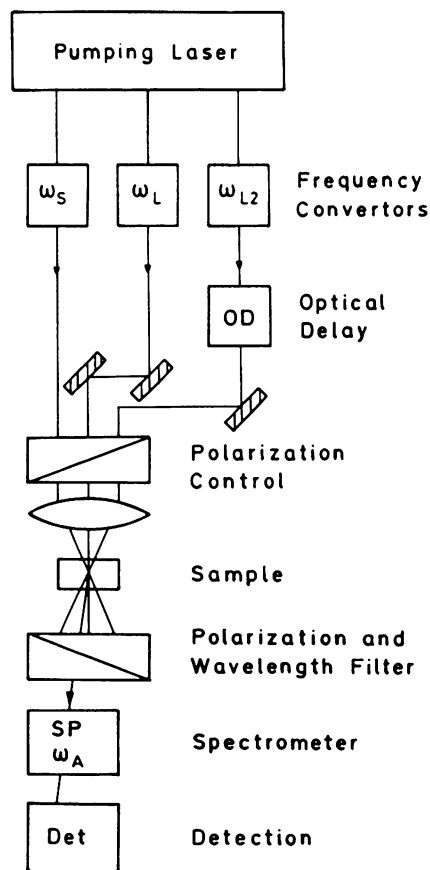


Fig.1 Schematic of the experimental system used to study time resolved coherent Raman spectroscopy. A mode-locked Ar-ion laser synchronously pumps dye lasers as frequency converters. The coherently scattered signal is recorded by a highly sensitive detection system

Fourier-transform coherent Raman experiment one works with the same Stokes pulses, but the exciting and probing laser pulses are very short, namely 60 fs. The latter are produced in a femtosecond unidirectional ring dye laser /13/. The exciting Stokes and laser pulses are focused into the sample generating the coherent material excitation. The probing pulses are delayed relative to the exciting pulses in the optical delay OD and then traverse (at the phase-matching angle) the excited volume of the sample. The weak coherently scattered light is separated from the incoming pulses via diaphragms, polarizers, and appropriate spectrometers. In the case of SEPI spectroscopy a high-resolution spectrograph ($\Delta\lambda/\lambda \approx 10^{-5}$) serves to observe the anti-Stokes spectrum. The detection system is a highly sensitive cooled photomultiplier.

4. Short Excitation and Prolonged Interrogation Spectroscopy of Hydrogen-bonded Aggregates

With the SEPI technique mixtures of liquid pyridine and methanol were studied. In these mixtures hydrogen bonds between pyridine and methanol occur, strongly influencing the spontaneous Raman spectra. In Fig.2 the spontaneous Raman data of pyridine:methanol mixtures are depicted for the spectral range of 980 cm^{-1} to 1030 cm^{-1} . In neat pyridine (lowest trace in Fig.2) the ν_1 mode occurs at 990.5 cm^{-1} . When methanol is added to pyridine, an additional broad band appears around 1000 cm^{-1} , which shifts with increasing methanol concentration /14/. Shoulders in the spontaneous Raman spectrum indicate that this band is made up of several components. The spontaneous Raman data do not allow to determine the number, the frequency positions, and the amplitudes of the different components. In Fig.3b and 3c we present SEPI data taken of two mixtures. For each mixture a dozen spectra were recorded. The laser frequency ω_L was kept constant and different anti-Stokes spectra were measured, when tuning the Stokes frequency in steps of 1 cm^{-1} . Of special interest are the narrow SEPI spectra around 1000 cm^{-1} . One finds two distinct bands at 997.3 cm^{-1} and at 1000 cm^{-1} , and a weaker component at 1001 cm^{-1} . The three frequency positions are marked in Fig.3 by vertical dash-dotted lines. The relative amplitudes of the two major components change considerably with concentration. While the component at 1000 cm^{-1} is strongest at $x_{py} = 0.33$ molar fraction (Fig.3b), one finds the component at 997.3 cm^{-1} to dominate at $x_{py} = 0.66$ molar fraction (Fig.3c). A large number of SEPI spectra was taken for

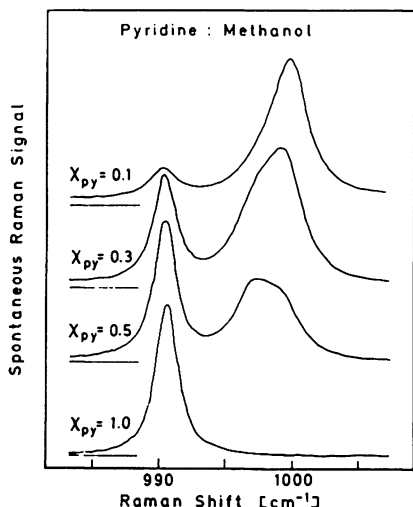


Fig. 2 Spontaneous Raman spectra of pure pyridine (lowest trace) and of mixtures of pyridine and methanol. In the mixtures a new band appears around 1000 cm^{-1} , which is due to complexes of pyridine and methanol. The band is resolved by SEPI spectroscopy into three lines (see Fig.3)

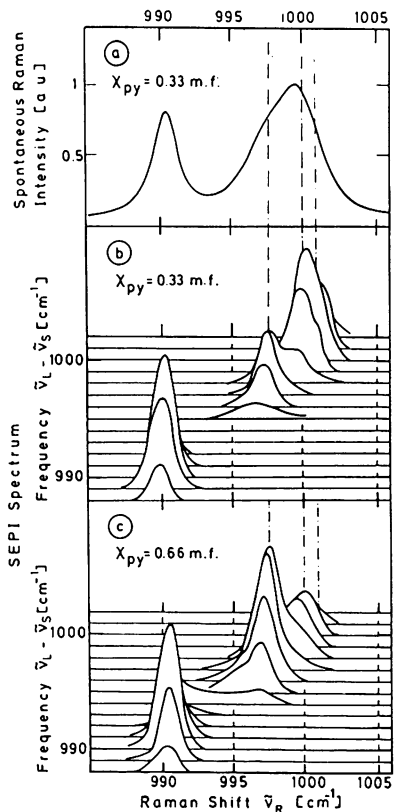
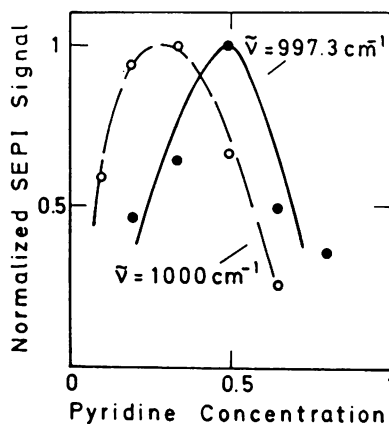


Fig. 3 Raman spectra of pyridine:methanol mixtures. (a) Polarized spontaneous Raman spectrum measured at a pyridine concentration of 0.33 molar fraction taken with a standard Raman spectrometer of spectral resolution of 0.5 cm^{-1} . (b) and (c) Short excitation and prolonged interrogation (SEPI) spectra obtained for a set of excitation frequencies $\tilde{\nu}_L - \tilde{\nu}_S$ at two pyridine concentrations, $x_{py} = 0.33$ molar fraction (b) and $x_{py} = 0.66$ molar fraction (c). The spectra, taken at excitation frequencies $\tilde{\nu}_L - \tilde{\nu}_S < 994 \text{ cm}^{-1}$, are drawn with reduced amplitudes [$\times 0.25$ in (b) and $\times 0.02$ in (c)]. The SEPI spectra resolve three Raman lines of different hydrogen-bonded aggregates hidden under the broad band of the spontaneous Raman spectrum (see dash dotted lines)

Fig. 4 Concentration dependences of the amplitudes of the two SEPI lines at 997.3 cm^{-1} and 1000 cm^{-1}



pyridine concentrations between $x_{py} = 0.1$ and 1.0 molar fraction. The concentration dependence of the amplitudes is shown in Fig.4 for the two SEPI lines at 997.3 cm^{-1} (full points) and 1000 cm^{-1} (circles). The band at 997.3 cm^{-1} rises to a peak value at $x_{py} = 0.5$ molar fraction, while the band at 1000 cm^{-1} shows a maximum at higher methanol concentrations with $x_{py} = 0.25$ molar fraction.

Our data suggest the following picture of the hydrogen bonded complexes: (i) There exist at least three distinct complexes of pyridine and methanol. (ii) The species at 997.3 cm^{-1} consists of one pyridine and one methanol molecule (PM). This complex has its highest concentration when pyridine and methanol are at equal numbers in the solution. (iii) The component at 1000 cm^{-1} appears to be made up of one pyridine and two or - more probably - four methanol molecules (PM_2 or PM_4). Indications for the latter complex are found in the literature; self-association of methanol is reported to occur at high methanol concentrations with a predominance of methanol tetramers /15/. (iv) The component at 1001 cm^{-1} is tentatively assigned to complexes PM_n with $n > 4$.

5. Fourier Transform Raman Spectroscopy of Transitions with Terahertz Frequency differences

High-resolution Fourier transform coherent Raman spectroscopy was first reported by Graener and Laubereau, who worked with light pulses of twenty picosecond duration. The authors studied vibrational-rotational transitions in CH_4 separated by less than 1 cm^{-1} with high resolution of 10^{-3} cm^{-1} . The data were taken in a time interval of 12 ns.

In this paper precise measurements are discussed of frequency differences between vibrational modes in liquids which are separated by tens to hundreds of wavenumbers. These large frequency differences may be studied in experiments which reveal the related beating phenomena. For example, a frequency difference of 200 cm^{-1} produces a beating pattern with peaks separated by 167 fs. In order to resolve this very short phenomenon, one has to work with femtosecond light pulses. Light pulses of approximately 50 fs duration became available only recently. We present two examples of time-resolved coherent Raman spectroscopy with femtosecond time resolution [16]. First we show data of pure liquid pyridine.

Liquid pyridine has Raman active vibrations at frequencies 991 cm^{-1} and 1030 cm^{-1} . They are assigned to two A_1 ring modes [17]. Both vibrations have similar spectral width (2.2 cm^{-1}) and similar Raman cross sections; they are separated by 39 cm^{-1} . In the Raman excitation process a frequency difference of $(\omega_L - \omega_S)/2\pi c = 1010 \text{ cm}^{-1}$ between the laser and the Stokes frequencies is applied. Due to the broad spectral width of the femtosecond exciting force of 200 cm^{-1} both pyridine modes are simultaneously excited in the experiment. Fig.5a shows the observed anti-Stokes signal plotted as a function of the time delay between

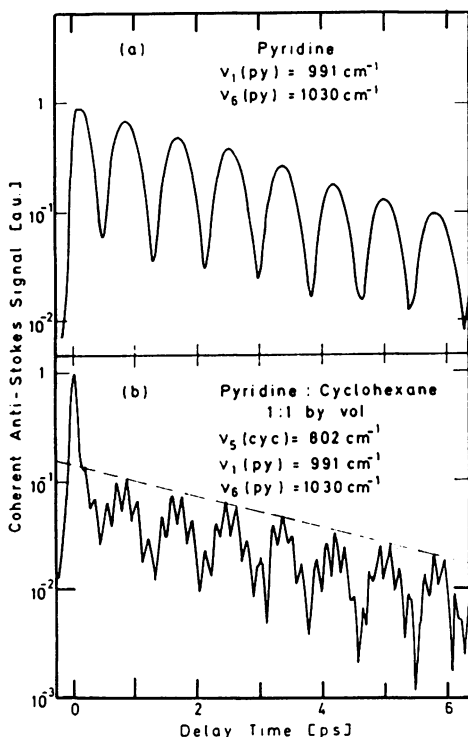


Fig.5 Time-resolved coherent Raman scattering using femtosecond time resolution. (a) Beat pattern resulting from pure pyridine after excitation of the two pyridine modes at 991 cm^{-1} and 1030 cm^{-1} . (b) Beat pattern recorded from a mixture of pyridine and cyclohexane. Beating of three molecular modes is observed

exciting and probing pulses. During the excitation process, at time zero, the coherent signal rises to a pronounced peak. It subsequently decays quickly over more than an order of magnitude. Later, the signal recovers and shows strong oscillations. The modulation depth exceeds a factor of ten. Two features of the coherent signal are of special interest here.

(i) The period of oscillation is 0.85 ps. Consequently, the frequency difference between the two modes is 1.175 ± 0.015 THz or $\Delta\tilde{\nu} = \Delta\nu/c = 39.2 \pm 0.5$ cm^{-1} . We emphasize that $\Delta\tilde{\nu}$ may be determined with high precision, mainly depending on the signal-to-noise ratio of the experiment and the accuracy of the optical delay line.

(ii) The envelope of the peaks of the oscillation decays exponentially with the decay time $T_2/2 = 2.55 \pm 0.15$ ps. The depths of the oscillations slightly decrease for long observation times, indicating a slight difference of 20% between the dephasing times of the two modes.

In Fig.5b we present an amazingly complicated but perfectly reproducible anti-Stokes pattern. A mixture of cyclohexane and pyridine (1:1 by volume) was investigated with femtosecond light pulses. (Note, that there are no hydrogen bonded aggregates in this mixture). In this case three vibrational modes with similar T_2 values beat together; they are: one cyclohexane mode at 802 cm^{-1} /18/ and the two pyridine modes at 991 cm^{-1} and 1030 cm^{-1} . We find a rich beating structure originating from the interference of the three modes.

The frequency differences of the investigated modes were determined by the following procedure. The exponential decay was removed by multiplying the signal with an exponential rising function. An appropriate window function was introduced to remove the influence of the boundaries of the time range. After these arithmetical manipulations a Fourier transformation of the time dependent data gave the results shown in Fig.6. Three sharp and pronounced peaks are found at 39 cm^{-1} , 189 cm^{-1} , and 228 cm^{-1} , which correspond to the frequency differences between the three modes excited in the mixture.

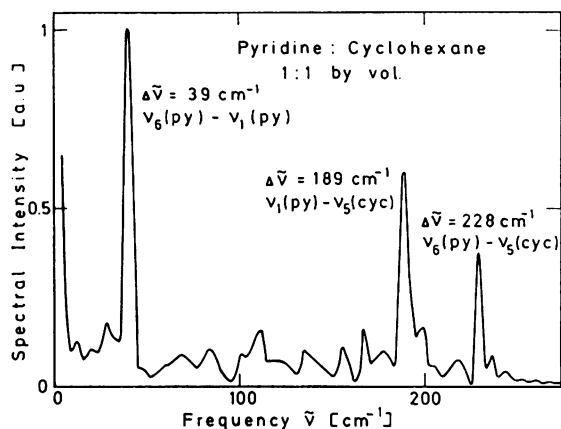


Fig. 6 Difference spectrum of pyridine and cyclohexane obtained by numerical Fourier transformation of the time resolved data from Fig.5b. Note the strong peaks at 39 cm^{-1} , 189 cm^{-1} , and 228 cm^{-1} , which correspond to the differences between the three excited modes. The highest difference frequency observed is $\Delta\nu = 6.84$ THz.

An important aspect remains to be discussed here: In order to improve spectral resolution in the time-domain experiment, the coherent signal has to be measured over delay times as long as possible. Taking into account the exponential decay of the signal, one immediately finds that the spectral resolution is directly related to the signal-to-noise ratio of the experiment. The following numbers should illustrate the situation. For dephasing times of approximately $T_2 = 3$ ps and with experimental data of the coherent Raman signal available over three orders of magnitude, one estimates an accuracy of the $\Delta\tilde{\nu}$ values of approximately 0.3 cm^{-1} .

6. Conclusions

We have shown that time resolved coherent Raman measurements provide spectral information hardly obtained from steady-state spontaneous spectra or from coherent steady-state spectroscopy. We have presented two different techniques which are of value in their own rights. The short excitation and prolonged interrogation (SEPI) technique is well adapted to resolve congested spectral regions; lines separated by a few wavenumbers are resolved. On the other hand, Fourier-transform coherent Raman spectroscopy using femtosecond light pulses is well suited to measure accurately frequency differences of modes separated by more than 200 cm^{-1} .

Acknowledgement

The authors acknowledge valuable contributions by M.C.Nuss, R.Leonhardt, W. Holzapfel, and R. Hackl at various stages of this work.

References

1. A. Laubereau, W. Kaiser: Rev. Mod. Phys. 50, 607 (1978);
A. Penzkofer, A. Laubereau, W. Kaiser: Progr. Quant. Electron. 6 55 (1979)
2. D. von der Linde, A. Laubereau, W. Kaiser: Phys. Rev. Lett. 26 954 (1971)
3. S. Velsko, J. Trout, R.M. Hochstrasser: J. Chem. Phys. 79, 2114 (1983)
4. G.M. Gale, P. Guyot-Sionnest, W.Q. Zheng: Optics Commun. 58, 395 (1986)
5. W. Zinth, W. Kaiser: In Organic Molecular Aggregates, eds. R.Reinecker, H.Haken, H.C.Wolf, Solid State Science, Vol.49, (Springer, New York 1983) p.124
6. H. Graener, A. Laubereau: Optics Commun. 54, 141 (1985)
7. R.L. Carman, I. Shimizu, C.S. Wang, N. Bloembergen: Phys. Rev. A2, 60 (1970)
8. W. Zinth, A. Laubereau, W. Kaiser: Optics Commun. 57, 457 (1978)
9. W. Zinth: Optics Commun. 34, 479 (1980)
10. W. Zinth, M.C. Nuss, W. Kaiser: Chem. Phys. Lett. 88, 257 (1982)
11. M.A. Collins, P.A. Madden, A.D. Buckingham: Chem. Phys. 24, 291 (1985)
12. W. Zinth, M.C. Nuss, W. Kaiser: Phys. Rev. A30, 1139 (1984)
13. J. Dobler, H.H. Schulz, W. Zinth: Optics Commun. 57, 407 (1986)
14. H. Takahashi, K. Mamola, E.K. Plyler, J. Mol. Spectrosc. 21, 217 (1966) B.P. Asthana, H. Takahashi, W. Kiefer: Chem. Phys. Lett. 94, 41 (1983)
15. W.B. Dixon: J. Phys. Chem. 74, 1396 (1970); A.N. Fletcher, *ibid.* 75, 1808 (1971)
16. R. Leonhardt, W. Holzapfel, W. Zinth, W. Kaiser: Chem. Phys. Lett., to be published 1987
17. D.A. Long, F.S. Murfin, E.L. Thomas, Trans. Farad. Soc. 59, 12 (1963)
18. K.B. Wiberg, A. Shrake: Spectrochim. Acta 27A, 1139 (1971)